nature climate change

ARTICLES

PUBLISHED ONLINE: 2 SEPTEMBER 2012 | DOI: 10.1038/NCLIMATE1664

Climate-change impact assessment for inlet-interrupted coastlines

Roshanka Ranasinghe[1,2,3]*, Trang Minh Duong[1,3], Stefan Uhlenbrook[1,2], Dano Roelvink[1,2] and Marcel Stive[2]

Climate-change (CC)-driven sea-level rise (SLR) will result in coastline retreat due to landward movement of the coastal profile (that is, the Bruun effect). Coastline change adjacent to commonly found tidal inlets will be influenced not only by the Bruun effect, but also by SLR-driven basin infilling and CC-driven variations in rainfall/runoff. However, as a model that accounts for all of the above-mentioned processes has been lacking so far, most coastal CC impact studies until now have considered only the Bruun effect. Here, we present a scale-aggregated model capable of providing rapid assessments of coastline change adjacent to small inlet-estuary/lagoon systems due to the combined effect of CC-driven SLR and variations in rainfall/runoff. Model applications to four representative systems show that the Bruun effect represents only 25–50% of total potential coastline change, and underline the significance of coastline change due to SLR-driven basin infilling and CC-driven variations in rainfall/runoff.

Most coastlines around the world are interrupted by inlets connecting the ocean to estuaries, lagoons and rivers[1–6]. For example, some 32,000 lagoons are reported along 13% of the world's coastline[2]. The total number of inlets in the world has not yet been quantified but is likely to run into thousands. Coastlines in the vicinity of inlets will not only be affected by CC-driven variations in oceanic processes[7–11] (for example, SLR) but also by CC-driven variations in terrestrial processes (for example, rainfall/runoff). Furthermore, coastal zones in the vicinity of inlets are commonly subjected to heavy human utilization (for example, for navigation, fishing and recreation). The combination of their sensitivity to multiple CC-driven variations in system forcing and their heavy human utilisation renders inlet-interrupted coasts highly vulnerable to CC impacts.

Scale-aggregated modelling is an effective approach to estimate the response of inlet-interrupted coasts to the combined effect of CC-driven SLR and variations in rainfall/runoff. This modelling approach does not include in-depth process descriptions (as in process-based models) nor promise highly accurate quantitative predictions, but adopts aggregated descriptions of system physics and delivers qualitatively correct estimates of system response to forcing. It is a fast modelling approach that enables multiple simulations, thereby facilitating probabilistic estimates of system response that are more useful for contemporary risk-based coastal management/planning frameworks than the single deterministic estimates usually provided by advanced process-based models. The application of the model ASMITA (Aggregated Scale Morphological Interaction between a Tidal basin and the Adjacent coast; refs 12,13) within the DIVA (Dynamic and Interactive Vulnerability Assessment) initiative[14,15] exemplifies the effective use of a scale-aggregated model to obtain regional-scale estimates of erosion (and other physical hazards) along the world's coastline. However, owing to the global coverage of DIVA, it has a very coarse resolution (the entire global coastline is discretized into just 12,148 elements with some elements exceeding 100 km) and therefore does not provide useful information for local-scale coastal management/planning[15,16]. Furthermore, although ASMITA provides an indication of whether sand will be exported or imported by the estuary/lagoon, it does not give any insights into exactly where the exported/imported sand will be deposited/borrowed from, and is therefore unable to provide direct estimates of local-scale coastline erosion/accretion.

In view of the high vulnerability of coastlines adjacent to inlets, an easy-to-use model capable of providing estimates of local-scale (<25 km alongshore) coastline change due to all relevant CC impacts (that is, both oceanic and terrestrial impacts) is urgently needed by front-line coastal managers/planners. The present study was undertaken with the specific aim of addressing this need.

The model

The CC-induced coastal response adjacent to an inlet is essentially a sediment budget issue, and is therefore dependent on the type of estuary/lagoon the inlet is connected to. The sediment supply/demand characteristics of tide-dominated estuaries, wave-dominated estuaries (also known as barrier or bar-built estuaries), barrier-island inlets (with no river flow) and lagoons can vary markedly[1,4]. For example, barrier-island coasts will experience barrier rollover due to SLR, thus reducing the tidal prism over time[17,18]; tide-dominated or mixed-energy coast inlets, where large ebb tidal deltas are usually present, are subject to complex ebb delta/inlet/estuary sand-transport mechanisms that may be modified nonlinearly by CC effects[3,13,19]; estuaries/lagoons backed by extensive salt marshes will increase their volume and thus tidal prisms (and inlet cross-section) owing to inundation of the salt marshes[4,18]. Thus, the development of a simple scale-aggregated model to simulate CC impacts on coastlines adjacent to all of these different types of inlet-estuary/lagoon system is beyond the scope of the present study. Therefore, here we focus on developing a

[1]Department of Water Engineering, UNESCO-IHE, PO Box 3015, 2601 DA Delft, The Netherlands, [2]Civil Engineering and Geosciences, Technical University of Delft, PO Box 5048, 2628 CN Delft, The Netherlands, [3]Harbour, Coastal and Offshore Engineering, Deltares, PO Box 177, 2600 MH Delft, The Netherlands. *e-mail: R.Ranasinghe@unesco-ihe.org.

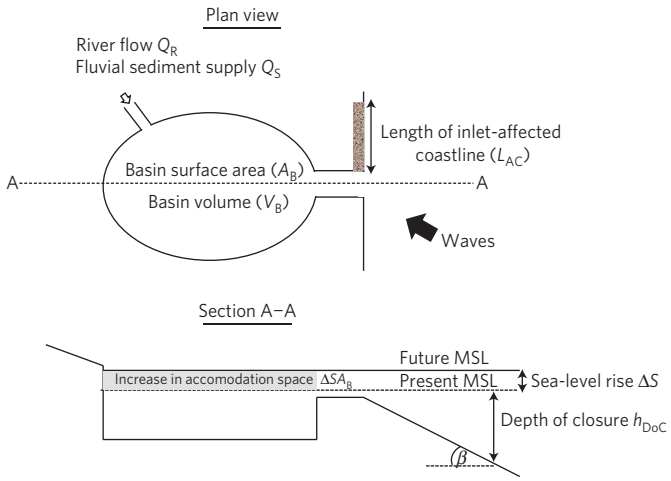

Figure 1 | Schematic showing the main parameters governing coastline change due to CC-driven SLR and variations in rainfall/runoff. MSL, mean sea level.

model that is suitable for one important and highly significant subcategory of inlet-estuary/lagoon systems; barrier estuaries. This type of system is predominantly found along sandy coasts located in wave-dominated, microtidal environments (~50% of the world's coastline[20,21]) and are also known as wave-dominated estuaries, bar-built estuaries, seasonally/intermittently open lagoons and small tidal inlets. Generally, they have little or no intertidal flats, backwater marshes or ebb tidal deltas[3,6]. The barrier is usually a sand spit that is connected to the mainland (as opposed to a barrier island that is completely separated from the mainland). Of the thousands of barrier estuaries around the world, many can be found along the west coast of USA, South Africa, the southeast and southwest coasts of Australia, Brazil and India[3,4,6,22]. Future, more advanced versions of the model are expected to relax this limit of applicability (to barrier estuaries) to eventually result in a generic model that is capable of providing rapid estimates of coastline change adjacent to all types of inlet-estuary/lagoon system.

Four main physical processes contribute to coastline change adjacent to barrier estuaries/lagoons (for convenience, a barrier estuary/lagoon is referred to as a basin herein): SLR-driven landward movement of the coastline (the Bruun effect), basin infilling due to the SLR-induced increase in basin accommodation space, basin volume change due to CC-driven increases/decreases in river flow, and increases/decreases in fluvial sediment supply. The methods adopted to incorporate these physical processes in the newly developed model are described below.

Bruun effect. The most well-known CC impact on coastlines is the SLR-driven upward and landward movement of the cross-shore coastal profile, resulting in coastline recession. This effect is referred to as the Bruun effect (ΔC_{BE}) and is commonly quantified using the Bruun rule[23], given as:

$$\Delta C_{BE} = \frac{\Delta S}{\tan\beta} \quad (1)$$

where ΔS is SLR (m) and $\tan\beta$ is the slope of the active profile (see Fig. 1 for parameter definitions).

However, a particular limitation of the Bruun rule is its non-applicability in the vicinity of coastal inlets where significant gradients in alongshore sediment transport prevail. This limitation of the Bruun rule was amply illustrated in ref. 24, where almost 70% of their 220-km-long study area (along the US east coast) had to be excluded, primarily owing to inlet influences.

SLR-driven basin infilling. In addition to the Bruun effect, inlet-interrupted coasts will also be affected by SLR-driven basin infilling[25]. The process of basin infilling due to SLR can be described as follows: SLR results in an increase in the basin volume below the mean water level. This additional volume is known as accommodation space. However, as the basin always tries to maintain an equilibrium volume, it will start importing sediment from offshore to raise the basin bed level such that the basin volume readjusts to its pre-SLR value. Depending on sediment availability, the basin will reach equilibrium when a sand volume equivalent to the SLR-induced accommodation space is imported into the basin. Thus, the basin infill volume is equal to the increase in accommodation space ΔSA_B, where A_B is the basin surface area (m^2). At the small inlet-basin systems considered herein, owing to the absence of pronounced ebb tidal deltas, this infill volume will be borrowed from the adjacent coastline, leading to a coastline recession of ΔC_{BI} (in addition to the recession due to the Bruun effect).

The additional recession due to basin infilling is accompanied by the landward shifting of the entire active coastal profile (that is, from the coastline to the depth of closure h_{DoC} (m)) along a certain alongshore length scale L_{AC} (that is, the length of the inlet-affected coastline (m)). Thus:

$$\Delta C_{BI} L_{AC} h_{DoC} = \Delta S A_B \quad (2)$$

However, owing to the different timescales associated with hydrodynamic forcing and morphological response, a potential lag exists between the rate of SLR and basin infilling[12]. By considering a linearized single-element version of ASMITA (which is valid for small inlet-basin systems), it can be shown that this lag effect can be represented by including a coefficient of about 0.5 in the right-hand side of equation (2) (see Supplementary Methods S1).

River flow-driven basin volume change. An inlet-basin system will strive to maintain cross-sectional equilibrium velocities[26,27]. Therefore, any CC-driven variation in the annual river flow (Q_R m^3 yr^{-1}) into the basin will result in an adjustment of the basin cross-section. In the small inlet-basin systems considered herein, this adjustment can safely be assumed to manifest itself through a deepening or raising of the bed. Using fundamental geometrical and physical considerations, the change in basin volume due to this process can be shown to be equal to $\Delta Q_R V_B/(P+Q_R)$, where Q_R is the present river flow into the basin during ebb (m^3), ΔQ_R is the CC-driven variation (from a baseline) in river flow during ebb (m^3), V_B is the present basin volume (m^3) and P is the mean ebb tidal prism (see Supplementary Methods S2). The denominator of the above term $(P+Q_R)$ accounts for the modification of the tidal prism due to river flow. An increase in Q_R (that is, positive ΔQ_R) will necessitate deepening of the basin and subsequently the basin volume will increase. The eroded sand will be supplied to the coastline adjacent to the inlet, or offset the amount of sand required from the coastline by the SLR-driven basin infilling process described above, thereby decreasing total coastline recession. A decrease in Q_R (that is, negative ΔQ_R) will necessitate raising of the basin bed and subsequently the basin volume will decrease. Owing to the absence of pronounced ebb deltas at the small inlet-basin systems considered herein, the sand required for this decrease in basin volume will also be borrowed from the coastline adjacent to the inlet, thereby augmenting the SLR-driven basin infilling process and increasing total coastline recession. As the coastline change due to this river flow-driven process (ΔC_{BV} (m)) will also occur on alongshore and cross-shore length scales relevant for ΔC_{BI}, it follows that:

$$\Delta C_{BV} L_{AC} h_{DoC} = \frac{\Delta Q_R V_B}{P+Q_R} \quad (3)$$

Table 1 | Study sites and their phenomenological classification.

System name	Location	CC-driven variation in rainfall/runoff	Inlet stability classification	Basin size*	Mean ebb tidal prism†	Rainfall magnitude‡	River flow magnitude§
Wilson inlet	Western Australia	Decrease	Seasonally closed	Small	Small	Low	Low
Swan River	Western Australia	Decrease	Permanently open	Large	Small	Low	Medium
Tu Hien inlet	North Vietnam	Increase	Intermittently closed	Medium	Medium	High	Medium
Thuan An inlet	North Vietnam	Increase	Permanently open	Medium	Large	High	High

*Basin size categories: small, $<100\times10^6$ m^3; medium, $100–200\times10^6$ m^3; large, $>200\times10^6$ m^3. †Tidal prism categories: small, $<10\times10^6$ m^3; medium, $10–25\times10^6$ m^3; large, $>25\times10^6$ m^3. ‡Rainfall categories: low, <1 m yr^{-1}; high, >1 m yr^{-1}. §River flow categories: low, $<500\times10^6$ m^3; medium, $500–1,000\times10^6$ m^3; high, $>1,000\times10^6$ m^3.

Table 2 | Model input parameter values.

System name	Basin area (km^2)	Basin volume (10^6 m^3)	Active profile slope (-)	Catchment area (km^2)	Length of affected coastline (km)	Mean ebb tidal prism (10^6 m^3)	Change in annual average river flow by 2100 (10^6 m^3 yr^{-1})	Change in annual average rainfall by 2100 (mm yr^{-1})
Wilson inlet	48	85	0.01	2,263	15	2.4	−60	−46.5
Swan River	52	312	0.01	121,000	20	2.6	−150	−43.5
Tu Hien inlet	100	122	0.01	600	10	15	120	495
Thuan An inlet	110	178	0.01	3,800	20	47	825	495

Table 3 | Model results.

System	Coastline change (m) due to worst-case CC-driven SLR		Coastline change (m) due to worst-case CC-driven variations in annual average rainfall/runoff		Total potential worst-case CC-driven coastline change (m) (ΔC_T)
	Bruun effect (ΔC_{BE})	Basin infill effect (ΔC_{BI})	Basin volume change effect (ΔC_{BV})	Fluvial sediment supply effect (ΔC_{FS})	
Wilson inlet	80	64	9	0	153
Swan River	80	52	48	0	180
Tu Hien inlet	80	266	−4	−2	340
Thuan An inlet	80	146	−7	−7	212

Rainfall/runoff-driven changes in fluvial sediment supply. Fluvial sediment supply (Q_s (m^3)) into a basin may change in the future owing to both natural processes and anthropogenic influences. The main natural processes that may result in significant changes in fluvial sediment supply are CC-driven variations in rainfall/runoff and natural changes in land cover (affecting the availability of erodible sediment). The main anthropogenic influences include upstream damming, changes in land use and environmental management practices.

Fluvial sediment supply to the basin may be estimated using the Universal Soil Loss Equation given by[28]:

$$A_{sl} = R_{sl} \times K_{sl} \times L_{sl} \times S_{sl} \times C_{sl} \times P_{sl} \quad (4)$$

where A_{sl} is the annual soil loss (m^3) per unit area in catchment, R_{sl} is the rainfall erosivity factor, K_{sl} is the soil erodibility factor, L_{sl} is the slope length factor, S_{sl} is the slope gradient factor, C_{sl} is the crop/vegetation management factor and P_{sl} is the support practice factor (all dimensionless).

The Universal Soil Loss Equation takes into account both CC-driven and anthropogenic influences on fluvial sediment supply. The CC-driven influences are mainly described by R_{sl} and to a lesser degree by K_{sl}, whereas anthropogenic influences are encapsulated by C_{sl} and P_{sl}. Q_s into a given basin can thus be estimated with:

$$Q_s = A_{sl} \times A_C \quad (5)$$

where A_C is the catchment area (m^2).

Owing to the relatively slow climatic change during the past few centuries, it is reasonable to assume that present-day inlet/basin systems are in a state of dynamic equilibrium where fluvial sediment supply is concerned. A relatively rapid change in Q_s due to accelerated CC in the future will disturb this equilibrium, leading to morphological changes in the basin. An increase in Q_s (that is, positive ΔQ_s) will reduce the sediment infill volume required from the coastline by basin infilling and/or basin volume change processes, thus decreasing net coastline recession. On the other hand, a decrease in Q_s (that is, negative ΔQ_s) will increase the sediment infill volume required from the coastline by the above basin processes, which will result in additional coastline recession. As the coastline change due to this process (ΔC_{FS} (m)) will also occur along the same alongshore and cross-shore length scales

relevant for ΔC_{BI} and ΔC_{BV}, it follows that

$$\Delta C_{FS} L_{AC} h_{DoC} = \int_0^T \Delta Q_S(t)\, dt \quad (6)$$

where t is time and T is the time duration being considered (in years).

Thus, the total potential coastline change due to CC-driven SLR and variations in rainfall/runoff is given by:

$$\Delta C_T = \Delta C_{BE} + \Delta C_{BI} + \Delta C_{BV} + \Delta C_{FS} \quad (7)$$

where ΔC_T is the total potential coastline recession (m).

It should be noted that equation (7) will provide a first estimate of the total potential coastline change due to the combined effects of CC-driven SLR and variations in rainfall/runoff. The actual coastline change may however depart from this potential magnitude owing to many reasons. For example, if the basin consists of a stiff clay bed (low erodibility) the actual increase in basin volume due to an increase in river flow might be significantly less than the potential value that will be calculated by equation (3), which will ultimately limit ΔC_T; availability of sand on the ocean side (for example, at nearshore zones consisting of non-erodible rock covered with a thin layer of sand) may also apply a limitation on the maximum ΔC_T possible (in this case equation (7) will overestimate coastline recession); and large volumes of sand entering embayed beaches through sporadic headland bypassing may also result in an actual ΔC_T value that is less than that given by equation (7).

Model applications and results

The newly developed model (equation (7)) was applied to four selected small inlet-basin systems to obtain first estimates of potential CC-driven coastline change by 2100. The study sites (Table 1 and Supplementary Table S1) were selected such that they represented seasonally, intermittently and permanently open inlet systems; small, medium and large basins and tidal prisms; low-, medium- and high-river flow conditions; and areas with both projected CC-driven increases and decreases in rainfall/runoff.

The model input parameters for each study site were obtained from published literature and/or using standard calculation methods (Table 2). For this preliminary application of the model, climate projections of SLR, rainfall and river flow reported in the Fourth Assessment Report of the Intergovernmental Panel on Climate Change[29] (which are derived from coarse-grid atmosphere ocean global circulation models) were directly adopted. Naturally, for local-scale applications that aim to obtain more accurate estimates of CC-driven coastal change, the model should be forced with higher-resolution downscaled climate projections. CC-driven variations in SLR, rainfall and runoff under high-end greenhouse-gas scenarios (for example A2, A1B) were used in this study to obtain worst-case-scenario estimates of potential coastline change.

The latest ensemble projections given in the Fourth Assessment Report of the Intergovernmental Panel on Climate Change (ref. 29) indicate that global average SLR could range between 0.18 and 0.79 m (including an allowance of 0.2 m for uncertainty associated with ice sheet flow[30]) by 2090–2099 relative to 1980–1999. Accordingly, an SLR of 0.8 m was specified in all model applications. Rainfall and runoff projections by 2100 for the A1B scenario at the study areas were determined from the ensemble projections given in ref. 31, Fig. 10.12 and ref. 32, Fig. 3.5, respectively.

Results. The computed values for the various terms in equation (7) for the study areas are given in Table 3. The relative contributions of the Bruun effect, the SLR-driven basin infilling effect and the rainfall/runoff effect are illustrated in Fig. 2 for two study areas (Tu Hien inlet, Vietnam and Swan River inlet, Western Australia, where future rainfall is projected to increase and decrease, respectively). These preliminary results provide several new insights regarding CC-driven coastline change adjacent to small inlet-basin systems. The most striking of these is that considering only the Bruun effect, as done in most local-scale coastal zone management/planning studies, will result in a considerable underestimation of coastline recession. For the four systems investigated, the coastline change due to the Bruun effect (ΔC_{BE}) represents only about 25–50% of the total potential coastline recession (first column of Table 4). The

Figure 2 | Model predicted coastline change by 2100 at Tu Hien inlet, VietNam and Swan River, Western Australia. a,**b**, Model-predicted coastline change by 2100 at Tu Hien inlet, Vietnam (projected increase in future rainfall; **a**) and Swan River, Western Australia (projected decrease in future rainfall; **b**). Purple line: Bruun effect alone (ΔC_{BE}); yellow line: Bruun effect and basin infilling combined (ΔC_{SLR}); red line: Bruun effect, basin infilling and rainfall/runoff effects combined (ΔC_T). Images adapted from Google Earth © 2012 Google.

Table 4 | Forcing contribution ratios.

System	$\Delta C_{BE}/\Delta C_T$ (%)	$\Delta C_{BI}/\Delta C_{BE}$ (%)	$\Delta C_{rainfall/runoff}/\Delta C_{BE}$ (%)
Wilson inlet	52	80	11
Swan River	44	65	60
Tu Hien inlet	23	333	−8
Thuan An inlet	37	183	−18

inclusion of just the basin infilling effect will increase the recession estimate by between 65% and 330% (second column of Table 4), compared with that due to the Bruun effect alone.

The model applications also indicate that CC-driven increases (decreases) in future rainfall/runoff will result in less (more) coastline recession. The magnitudes of coastline change due to CC-driven variations in rainfall/runoff ($\Delta C_{\text{rainfall/runoff}} = \Delta C_{\text{BV}} + \Delta C_{\text{FS}}$) relative to those due to the Bruun effect alone (ΔC_{BE}) are shown in Table 4 (third column). These results indicate that the range of increases (decreases) in recession due to worst-case CC-driven decreases (increases) in rainfall/runoff are between 11% and 60% (8% and 18%) of the Bruun effect. The over/underestimates of total potential coastline change that result from the non-consideration of rainfall/runoff effects is greater for systems with a high basin volume/(tidal prism + river flow) ratio (for example, 27% underestimate at Swan river).

It should be noted that the model and results presented above consider only the effects of CC-driven variations in annual average rainfall/runoff. CC is also expected to affect the frequency and intensity of extreme rainfall/runoff events that may result in irreversible episodic effects (for example, breaching of new inlets, bifurcation of ebb/flood deltas). Such effects cannot be adequately represented solely by the scale-aggregated modelling approach adopted here, and require strategic input from process-based coupled hydrological/morphodynamic modelling.

Conclusions

A new physically based, scale-aggregated model to obtain rapid estimates of potential coastline change due to the combined effects of CC-driven SLR and variations in rainfall/runoff is developed. The model is particularly suited to assess CC-driven coastline change along coastlines adjacent to the thousands of highly vulnerable small inlet-basin systems around the world.

The model was applied to four representative small inlet-basin systems to obtain preliminary estimates of potential CC-driven coastline change by 2100. The selected study sites span a sufficiently wide parameter space in relation to the present-day inlet condition, basin size, river flow, tidal prism, and projected CC-driven variations in rainfall/runoff (increases and decreases).

Model results indicate that coastline change due to SLR-driven basin infilling and CC-driven variations in rainfall/runoff can be very significant along coastlines adjacent to small inlet-basin systems and therefore cannot be neglected. Considering only the Bruun effect, as commonly done, can lead to misleading coastline change estimates that are inappropriate for coastal zone management/planning decisions. At the selected study sites, coastline change due to the Bruun effect represents only about 25–50% of the total potential coastline recession.

Received 3 October 2011; accepted 19 July 2012; published online 2 September 2012

References

1. Aubrey, D. G. & Weishar, L. *Hydrodynamics and Sediment Dynamics of Tidal Inlets* (Springer, 1988).
2. Carter, R. W. G. & Woodroffe, C. D. *Coastal Evolution: Late Quaternary Shoreline Morphodynamics* (Cambridge Univ. Press, 1994).
3. Woodroffe, C. D. *Coasts: Form, Process and Evolution* (Cambridge Univ. Press, 2002).
4. Davis, R. Jr & Fitzerald, D. M. *Beaches and Coasts* (Wiley, 2009).
5. Ward, L. G. & Ashley, G. M. *Physical Processes and Sedimentology of Siliciclastic-dominated Lagoonal Systems* (Elsevier, 1989).
6. Kjerfve, B. in *Coastal Lagoon Process* (ed. Kjerfve, B.) 1–7 (Elsevier, 1994).
7. Nicholls, R. J. *et al.* in *IPCC Climate Change 2007: Impacts, Adaptation and Vulnerability* (eds Parry, M. L. *et al.*) 315–317 (Cambridge Univ. Press, 2007).
8. Ranasinghe, R. & Stive, M. J. F. Rising seas and retreating coastlines. *Climatic Change* **97,** 465–468 (2009).
9. Stive, M. J. F., Ranasinghe, R. & Cowell, P. in *Handbook of Coastal and Ocean Engineering* (ed. Kim, Y.) 1023–1038 (World Scientific, 2010).
10. Houghton, K. J, Vafeidis, A. T., Neumann, B. & Proelss, A. Maritime boundaries in a rising sea. *Nature Geosci.* **3,** 813–186 (2010).
11. Gratiot, N. *et al.* Significant contribution of the 18.6 year tidal cycle to regional coastal changes. *Nature Geosci.* **1,** 169–172 (2008).
12. Stive, M. J. F., Capobianco, M., Wang, Z. B., Ruol, P. & Buijsman, M. C. *Proc. 8th Int. Biennial Conf. on Physics of Estuaries and Coastal Seas, The Hague* 397–407 (A. A. Balkema, 1998).
13. Van Goor, M. A., Stive, M. J. F., Wang, Z. B. & Zitman, T. J. Impact of sea level rise on the morphological stability of tidal inlets. *Marine Geol.* **202,** 211–227 (2003).
14. Hinkel, J. DIVA: An iterative method for building modular integrated models. *Adv. Geosci.* **4,** 45–50 (2005).
15. Hinkel, J. & Klein, R. J. T. The DINAS-COAST project: Developing a tool for the dynamic and interactive assessment of coastal vulnerability. *Glob. Environ. Change* **19,** 384–395 (2009).
16. Vafeidis, A. T. *et al.* A new global coastal database for impact and vulnerability analysis to sea-level rise. *J. Coast. Res.* **24,** 917–924 (2008).
17. Dean, R.G. & Maurmeyer, E.M. in *Handbook of Coastal Processes and Erosion Boca Raton* (ed. Komar, P. D.) 151–166 (CRC, 1983).
18. FitzGerald, D. M., Fenster, M. S., Argow, B. A. & Buynevich, I. V. Coastal impacts due to sea-level rise. *Annu. Rev. Earth Planet. Sci.* **36,** 601–647 (2008).
19. Walton, T. L. & Adams, W. D. *Proc. 15th Coastal Engineering Conf., Honolulu* 1919–1937 (ASCE, 1976).
20. Davies, J. L. *Geographical Variation in Coastal Development* (Longman, 1980).
21. Davis, R. A. & Hayes, M. O. What is a wave dominated coast. *Marine Geol.* **60,** 313–329 (1984).
22. Ranasinghe, R., Pattiaratchi, C. & Masselink, G. A morphodynamic model to simulate the seasonal closure of tidal inlets. *Coast. Eng.* **37,** 1–36 (1999).
23. Bruun, P. Sea-level rise as a cause of shore erosion. *J. Waterways Harbors Div.* **88,** 117–130 (1962).
24. Zhang, K., Douglas, B. & Leatherman, S. Global warming and coastal erosion. *Climatic Change* **64,** 41–58 (2004).
25. Stive, M. J. F. & Wang, Z. B. in *Advances in Coastal Modelling* (ed. Lakhan, C.) 367–392 (Elsevier, 2003).
26. O'Brien, M. P. Estuary and tidal prisms related to entrance areas. *Civil Eng.* **1,** 738–739 (1931).
27. Van der Wegen, M., Dastgheib, A. & Roelvink, J. Morphodynamic modelling of tidal channel evolution in comparison to empirical PA relationship. *Coast. Eng.* **57,** 827–837 (2010).
28. Wischmeier, W. & Smith, D. *Agricultural Handbook No. 537* (US Government Printing Office, 1978).
29. Alley, R. B. *et al.* in *Climate Change 2007: The Physical Science Basis* (eds Solomon, S. *et al.*) 1–18 (Cambridge Univ. Press, 2007).
30. Schoof, C. Ice-sheet acceleration driven by melt supply variability. *Nature* **468,** 803–806 (2010).
31. Solomon, S. *et al.* in *IPCC Climate Change 2007: The Physical Science Basis* (eds Solomon, S. *et al.*) 19–92 (Cambridge Univ. Press, 2007).
32. IPCC *Climate Change 2007: Synthesis Report* (eds Pachauri, R. K. and Reisinger, A.) (IPCC, 2007).

Acknowledgements

Z. B. Wang (Deltares/Delft University of Technology) is gratefully acknowledged for providing invaluable advice and guidance on the SLR-driven basin infilling process and the ASMITA model. R.R. would like to thank J. Bosboom (Delft University of Technology) and Ad van der Spek (Deltares) for early discussions pertaining to this research. This study was partly supported by the Deltares Coastal Maintenance Research Programme Beheer and Onderhoud Kust.

Author contributions

R.R. and M.S. conceived the idea of the new model. R.R. developed and tested the model and wrote the manuscript. T.M.D. collated model input data and applied the model to field sites. S.U. provided all hydrological analysis for this study. D.R. provided strategic advice on coastal processes. All authors provided suggestions and comments on the manuscript.

Additional information

Supplementary information is available in the online version of the paper. Reprints and permissions information is available online at www.nature.com/reprints. Correspondence and requests for materials should be addressed to R.R.

Competing financial interests

The authors declare no competing financial interests.